NIH Public Access
Author Manuscript
J Neurosci. Author manuscript; available in PMC 2010 August 12.

Published in final edited form as:
J Neurosci. 2009 August 12; 29(32): 10171–10179. doi:10.1523/JNEUROSCI.1300-09.2009.

Functional connectivity delineates distinct roles of the inferior frontal cortex and pre-supplementary motor area in stop signal inhibition

Jeng-Ren Duann[1], **Jaime S. Ide**[2], **Xi Luo**[2,3], and **Chiang-shan Ray Li**[2,4,5,*]

[1] Swartz Center for Computational Neuroscience, Institute of Neural Computation, University of California, San Diego, CA 92093

[2]Department of Psychiatry, Yale University, New Haven, CT 06519

[3]Department of Statistics, Yale University, New Haven, CT 06519

[4]Department of Neurobiology, Yale University, New Haven, CT 06519

[5]Interdepartmental Neuroscience Program, Yale University, New Haven, CT 06519

Abstract

The neural basis of motor response inhibition has drawn considerable attention in recent imaging literature. Many studies have employed the go/no-go or stop signal task to examine the neural processes underlying motor response inhibition. In particular, showing greater activity during no-go (stop) as compared to go trials and during stop success as compared to stop error trials, the right inferior prefrontal cortex (IFC) has been suggested by numerous studies as the cortical area mediating response inhibition. Many of these same studies as well as others have also implicated the pre-supplementary motor area (preSMA) in this process, in accord with a function of the medial prefrontal cortex in goal-directed action. Here we employed connectivity analyses to delineate the roles of IFC and preSMA during stop signal inhibition. Specifically, we hypothesized that, as an integral part of the ventral attention system, the IFC responds to a stop signal and expedites the stop process in the preSMA, the primary site of motor response inhibition. This hypothesis predicted that preSMA and primary motor cortex would show functional interconnectivity via the basal ganglia circuitry to mediate response execution or inhibition, whereas the IFC would influence the basal ganglia circuitry via connectivity with preSMA. The results of Granger causality analyses in 57 participants confirmed this hypothesis. Furthermore, psychophysiological interaction showed that, as compared to stop errors, stop successes evoked greater effective connectivity between the IFC and preSMA, providing additional support for this hypothesis. These new findings provided evidence critically differentiating the roles of IFC and preSMA during stop signal inhibition and have important implications for our understanding of the component processes of inhibitory control.

Keywords

ventral attention system; impulsivity; no-go; neuroimaging; inhibitory control; prefrontal; PPI

*Address correspondence to: Dr. Chiang-shan Ray Li Connecticut Mental Health Center, S103 Department of Psychiatry, Yale University School of Medicine 34 Park Street New Haven, CT 06519 Phone: 203-974-7354 FAX: 203-974-7076 chiang-shan.li@yale.edu.

Introduction

The go/no-go and stop signal task (SST) have been widely used to investigate the behavioral and neural processes of motor response inhibition (Logan and Cowan, 1984). In these behavioral tasks, a "go" stimulus required participants to respond within a time window. Because these go trials occur most of the time, they set up a prepotent response tendency. In contrast, the stop signal instructs participants to withhold their response. The rationale is that, when response inhibition is in place, participants are able to stop upon seeing the stop signal. Thus, many previous studies have compared stop success with stop error trials or simply stop trials with go trials and identified bilateral or right inferior prefrontal cortex (IFC) as a cortical site of inhibitory motor control (Verbruggen and Logan, 2008). It was theorized that the IFC projects to the subthalamic nucleus (STN) in a hyper-direct pathway for motor inhibitory control (Aron and Poldrack, 2006).

Many of these and other studies have also isolated the pre-supplementary motor area (preSMA) as a key locus of response inhibition, in keeping with a role of this medial prefrontal structure in action control and selection (Nachev et al., 2008). In particular, greater preSMA activation was associated with shorter stop signal reaction time, an index of inhibitory control as computed on the basis of the race model (Li et al., 2006a). An important question is thus whether the IFC and preSMA play a similar or different role in motor response inhibition.

The extensive literature has suggested that the IFC is part of the ventral attention system, which activates in response to the detection of a salient target, particularly when the target is behaviorally relevant (Bledowski et al., 2004; Corbetta et al., 2008; Corbetta and Shulman, 2002; Hampshire et al., 2009). For instance, in spatial cueing paradigms the right IFC along with the temporal parietal junction responds and reorients attention to an external stimulus that occurs unexpectedly or infrequently, when the stimulus is a target (Kincade et al., 2005; Serences et al., 2005). In the stop signal task, the stop signal is both infrequent and behaviorally relevant. Thus, greater IFC activity during stop as compared to go trials may simply reflect attentional processing of the stop signal. By increasing activity in response to the stop signal, the IFC may serve to orient attention and resources to the stop process and, as a result, facilitate stop signal inhibition.

The current study aimed to substantiate these roles of the IFC and preSMA in stop signal inhibition. We hypothesized that the IFC would facilitate stop signal inhibition via functional connectivity with the preSMA, and sought to confirm this hypothesis with Granger causality analysis (GCA). Specifically, we predicted that the preSMA and primary motor cortex would show strong interconnectivity with the basal ganglia circuitry of motor control, to determine the outcome of go and stop processes, whereas the IFC would indirectly influence the basal ganglia circuitry via connectivity with preSMA. We also predicted that, in psychophysiological interaction (PPI, Friston et al., 1997; Gitelman et al., 2003), stop success would evoke greater effective connectivity between the IFC and preSMA, as compared to stop error trials.

Materials and Methods

Subjects and behavioral task

Sixty subjects (30 men, 22-45 years of age, all right-handed) were paid to participate in the study. All subjects signed a written consent after details of the study were explained, in accordance to institute guidelines and procedures approved by the Yale Human Investigation Committee.

We employed a simple reaction time task in this stop-signal paradigm (Li et al., 2006a; 2008a; 2008b; Logan and Cowan, 1984). There were two trial types: "go" and "stop," randomly intermixed. A small dot appeared on the screen to engage attention at the beginning of a go trial. After a randomized time interval (fore-period) between 1 and 5 s, the dot turned into a circle (the "go" signal), which served as an imperative stimulus, prompting the subjects to quickly press a button. The circle vanished at a button press or after 1 s had elapsed, whichever came first, and the trial terminated. A premature button press prior to the appearance of the circle also terminated the trial. Three quarters of all trials were go trials. The remaining one quarter were stop trials. In a stop trial, an additional "X," the "stop" signal, appeared after and replaced the go signal. The subjects were told to withhold button press upon seeing the stop signal. Likewise, a trial terminated at button press or when 1 s had elapsed since the appearance of the stop signal. The stop signal delay (SSD) – the time interval between the go and stop signal – started at 200 ms and varied from one stop trial to the next according to a staircase procedure: if the subject succeeded in withholding the response, the SSD increased by 64 ms; conversely, if they failed, SSD decreased by 64 ms (De Jong et al., 1990; Levitt, 1970). There was an inter-trial-interval of 2 s. Subjects were instructed to respond to the go signal quickly while keeping in mind that a stop signal could come up in a small number of trials. Prior to the fMRI study each subject had a practice session outside the scanner. In the scanner each subject completed four 10-min runs of the task with the SSD updated manually across runs. Depending on the actual stimulus timing (trials varied in fore-period duration) and speed of response, the total number of trials varied slightly across subjects in an experiment. With the staircase procedure we anticipated that the subjects would succeed in withholding their response in approximately half of the stop trials.

We computed a critical SSD that represents the time delay between go and stop signals that a subject would require in order to succeed in 50% of the stop trials (Levitt, 1970). Specifically, SSDs across trials were grouped into runs, with each run being defined as a monotonically increasing or decreasing series. We derived a mid-run estimate by taking the middle SSD (or average of the two middle SSDs if there was an even number of SSDs) of every second run. The critical SSD was computed by taking the mean of all mid-run SSDs. It was reported that, except for experiments with a small number of trials (less than 30), the mid-run estimate was close to the maximum likelihood estimate of X_{50} (50% positive response; i.e., 50% SS in the SST, Wetherill et al., 1966). The stop signal reaction time (SSRT) was computed by subtracting the critical SSD from the median go trial RT (Logan, 1994).

Thirty subjects were also imaged in a 10-minute "resting state" session, in which they were instructed to stay awake and relaxed, with their eyes closed.

Imaging protocol

Conventional T_1-weighted spin echo sagittal anatomical images were acquired for slice localization using a 3T scanner (Siemens Trio). Anatomical images of the functional slice locations were next obtained with spin echo imaging in the axial plane parallel to the AC-PC line with TR = 300 ms, TE = 2.5 ms, bandwidth = 300 Hz/pixel, flip angle = 60°, field of view = 220 × 220 mm, matrix = 256 × 256, 32 slices with slice thickness = 4mm and no gap. Functional, blood oxygenation level dependent (BOLD) signals were then acquired with a single-shot gradient echo echoplanar imaging (EPI) sequence. Thirty-two axial slices parallel to the AC-PC line covering the whole brain were acquired with TR = 2,000 ms, TE = 25 ms, bandwidth = 2004 Hz/pixel, flip angle = 85°, field of view = 220 × 220 mm, matrix = 64 × 64, 32 slices with slice thickness = 4mm and no gap. Three hundred images were acquired in each run for a total of four runs.

Spatial preprocessing and general linear modeling

Data were analyzed with Statistical Parametric Mapping version 5 (SPM5, Wellcome Department of Imaging Neuroscience, University College London, U.K.). Images from the first five TRs at the beginning of each trial were discarded to enable the signal to achieve steady-state equilibrium between RF pulsing and relaxation. Images of each individual subject were first corrected for slice timing, realigned (motion-corrected) and unwarped (Andersson et al. 2001; Hutton et al., 2002). A mean functional image volume was constructed for each subject for each run from the realigned image volumes. These mean images were normalized to an MNI (Montreal Neurological Institute) EPI template with affine registration followed by nonlinear transformation (Ashburner and Friston, 1999; Friston et al., 1995a). The normalization parameters determined for the mean functional volume were then applied to the corresponding functional image volumes for each subject. Finally, images were smoothed with a Gaussian kernel of 10 mm at Full Width at Half Maximum.

Statistical modeling of the imaging data was described in detail in our earlier studies (Li et al., 2006a; 2008a; 2008b). Briefly, four main types of trial outcome were distinguished: go success (G), go error (F), stop success (SS), and stop error (SE) trial. An analytical statistical design was constructed for each individual subject, using the general linear model (GLM) with the onsets of go signal in each of these trial types convolved with a canonical hemodynamic response function (HRF) and with the temporal derivative of the canonical HRF entered as regressors in the model (Friston et al., 1995b). Realignment parameters in all six dimensions were also entered in the model. The data were high-pass filtered (128 s cutoff) to remove low-frequency signal drifts. Serial autocorrelation was corrected by a first-degree autoregressive or AR(1) model. In the first-level analysis, we constructed for each individual subject a contrast between SS and SE. The *con* or contrast (difference in β) images of the first-level analysis were then used for the second-level group statistics (random effect analysis; Penny and Holmes, 2004). Brain regions were identified using an atlas (Duvernoy, 1999; Mai et al., 2003). All templates are in MNI space and voxel activations are presented in MNI coordinates. We used MarsBaR to derive for each individual subject the effect size of activity change for regions of interest (Brett et al., 2002; http://marsbar.sourceforge.net/).

Granger causality analysis (GCA)

Task-related and resting state time series were examined with GCA of multivariate autoregressive models (Granger, 1969), a method widely used to describe "causal" influence between sets of EEG or fMRI time series (Ding et al., 2000; Kaminski et al., 2001; Goebel et al., 2003; Kus et al., 2004; Roebroeck et al., 2005; Sato et al., 2007; Deshpande et al., 2009). In this analysis, we included as regions of interest (ROI) the preSMA, rIFC, and primary motor cortex (PMC), caudate head, and the subthalamic nucleus (STN). The masks of preSMA, rIFC, and PMC were derived on the basis of regional brain activations obtained in Li et al., 2006a. The MNI coordinates of these three structures were x=−4, y=36, z=56 (preSMA); x=44, y=48, z=−12 (rIFC); and x=−36, y=−8, z=52 (PMC). We included in the model the left caudate head, which showed greater activation in association with short stop signal reaction time (Li et al., 2008b). Masks of the left caudate head and the STN were obtained from the AAL atlas (Tzourio-Mazoyer et al., 2002).

The application of multivariate autoregressive modeling requires that each ROI time-series is covariance stationary, which we examined with the Augmented Dickey Fuller (ADF) test (Hamilton, 1994). ADF test verified that there is no unit root in the time-series. BOLD time series were concatenated across all four sessions for each individual subject. The data of 57 of the 60 subjects were covariance stationary and subjected to GCA.

The preprocessed BOLD time series were averaged for each subject across all voxels in each of the five ROIs. In a multi-dimensional vector autoregressive (VAR) model (Goebel et al., 2003; Sato et al., 2006; Seth and Edelman, 2007) we computed the Granger causality (G-causality) between the time series

$$\begin{bmatrix} x_{1,t} \\ x_{2,t} \\ \vdots \\ x_{5,t} \end{bmatrix} = \begin{bmatrix} \mu_1 \\ \mu_2 \\ \vdots \\ \mu_5 \end{bmatrix} + \begin{bmatrix} A_{11}^1 & A_{12}^1 & \cdots & A_{15}^1 \\ A_{21}^1 & A_{22}^1 & \cdots & A_{25}^1 \\ \vdots & \vdots & \ddots & \vdots \\ A_{51}^1 & A_{52}^1 & \cdots & A_{55}^1 \end{bmatrix} \begin{bmatrix} x_{1,t-1} \\ x_{2,t-1} \\ \vdots \\ x_{5,t-1} \end{bmatrix} + \cdots + \begin{bmatrix} A_{11}^k & A_{12}^k & \cdots & A_{15}^k \\ A_{21}^k & A_{22}^k & \cdots & A_{25}^k \\ \vdots & \vdots & \ddots & \vdots \\ A_{51}^k & A_{52}^k & \cdots & A_{55}^k \end{bmatrix} \begin{bmatrix} x_{1,t-k} \\ x_{2,t-k} \\ \vdots \\ x_{5,t-k} \end{bmatrix} + \begin{bmatrix} \mu_1 \\ \mu_2 \\ \vdots \\ \mu_5 \end{bmatrix} \quad (1)$$

assuming that

$$\Sigma_u = \begin{bmatrix} \Sigma_{11} & \Sigma_{12} & \cdots & \Sigma_{15} \\ \Sigma_{21} & \Sigma_{22} & \cdots & \Sigma_{25} \\ \vdots & \vdots & \ddots & \vdots \\ \Sigma_{51} & \Sigma_{52} & \cdots & \Sigma_{55} \end{bmatrix} \quad (2)$$

In Equation 1, $x_{i,t}$, i=1, 2, ..., 5 represent the time series of IFC, preSMA, PMC, caudate head, and STN respectively, with $x_{i,t}$ and $x_{i,t-p}$ representing the value of the time series at time t and time t-p, respectively, and p=1,2,...,k, where k is the order of the VAR model. The optimal time lag was determined using Akaike information criterion (AIC, Akaike, 1974). Also, μ_i (i=1, 2, ..., 5) are the means of the five time series and $A_{i,j}^p$, where i,j = 1, 2,..., 5, and p=1, 2,..., k, are the linear coefficients of the VAR model (i.e., the contributions of each "lagged" observation to the predicted values of $x_{i,t}$). u_i (i=1, 2,..., 5) are the residuals (prediction errors) for each of the time series, which were assumed to have a Gaussian distribution, N(0,Σ_u) (Equation 2).

Time series x_1 is said to be "Granger-caused" (or G-caused) by time series x_2 if the inclusion of time series x_2 reduces the variance of the residual (Σ_{12} in Equation 2) obtained by the autoregressive model of time series x_1 itself (Σ_{11}, Granger, 1969). We tested the significance of the G-causality between time series x_1 and x_2 by an F-test:

$$S = \frac{\left(\sum_{i=1}^{T} \Sigma_{11}^i - \sum_{i=1}^{T} \Sigma_{12}^i\right) / p}{\sum_{i=1}^{T} \Sigma_{12}^i / (T - 2p - 1)} \sim F_{p,T-2p-1} \quad (3)$$

where T is the total number of time points and p is the order of the VAR model. If the test statistic of Equation 3 was greater than a specified significance criterion (e.g., p<0.0025, correcting for a total of 20 comparisons for each subject), we rejected the NULL hypothesis that time series x_2 did not G-cause time series x_1 (Geweke, 1982). Note that it is not necessary that time series x_1 and x_2 have reciprocal G-causality. The direction of G-causality between time series x_1 and x_2 is determined by the residual variance Σ_{12} and Σ_{21} , and these two terms may not be identical as they are derived by two different regression estimations.

Because we used a multi-dimensional VAR model, we could determine all the residual terms in a single model, and, importantly, identified if there was an intermediate node between two target nodes. That is, a multi-dimensional model helped differentiate the G-causality between X -> Y and X -> Z -> Y, which would be identical if a bivariate approach was used (Geweke, 1982).

We determined the G-causalities of the five time series for individual subjects, correcting for multiple comparisons (p<0.05/20=0.0025) and computed the significance of the effective connectivity for the entire sample using a binomial test. In an alternative analysis, we determined the G-causalities for individual subjects by bootstrapping from the data time series of the five ROIs, prior to group analysis with the binomial test (see below).

Psychophysiological Interaction

Psychophysiological interaction (PPI) describes how functional connectivity between brain regions is altered as a result of psychological context or variables (Friston et al., 1997; Gitelman et al., 2003). In pursuit of our hypothesis that the IFC is functionally connected with the preSMA to expedite stop signal inhibition, we anticipated greater connectivity between the two brain regions during stop success (SS) as compared to stop error (SE) trials.

The time-series of the first eigenvariate of the BOLD signal were temporally filtered and mean corrected, and deconvolved to generate the time series of the neuronal signal for the source region – the IFC – as the physiological variable in the PPI. The psychological variable represented the contrast between SS and SE trials: SS minus SE. An additional regressor represented the interaction between the psychological and physiological factors. These regressors were convolved with the canonical hemodynamic response function (HRF) and entered into the regression model. The interaction term in the resulting SPM showed areas with significant differential connectivity to the IFC because of the psychological context “SS minus SE”. PPI analysis was carried out for each subject and the resulting images of contrast estimates were used for random effect group analysis.

Results

Stop signal performance

Subjects had a mean go trial success rate of 96.1 (± 4.2) % (mean ± standard deviation, across subjects) with a median RT of 557 (± 120) ms. The average stop success rate was 50.5 (± 2.4) %, suggesting that their performance was adequately tracked by the staircase procedure. The average stop signal reaction time was 205 (± 38) ms, well in the range of the values reported in numerous previous studies (Tseng and Li, 2008).

Regional brain activations during stop signal performance

We examined regional brain activation associated with stop signal inhibition, using the same analyses as in our previous studies (Li et al., 2006a; 2008c). The results of the current cohort of 57 subjects confirmed our previous findings. Compared to stop error (SE), stop success (SS) trials evoked greater activation in bilateral superior/middle and inferior frontal cortices. In contrast, compared to SS, SE trials evoked greater activation in many cortical and subcortical structures including the dorsal anterior cingulate cortex (ACC) and the thalamus (Supplementary Figure 1). Furthermore, on the basis of a median split of the SSRT, we compared 28 subjects with short to the other 28 with long SSRT (174 ± 23 ms vs. 235 ± 28 ms, $p<0.0001$) and observed greater activation in a dorsomedial region of the superior frontal cortex and a sub-region in the rostral ACC (Supplementary Figure 2).

Granger causality analysis (GCA)

The results of GCA of the stop signal task time series showed that the preSMA and PMC have significant connectivity with the caudate head and STN and that the IFC projected to the preSMA but not to the basal ganglia ($p<0.0025$, corrected for multiple comparisons, for individual GCA; $p<0.01$, binomial test for group analysis; Table 1a; Fig. 1). With $p<0.05$, the binomial test for group results showed that the IFC and preSMA are reciprocally connected. In contrast, no significant Granger causality was observed for any of the connections for the resting state time series (Table 1b).

To further confirm these results, we employed GCA on time series re-sampled ("bootstrapped") from our data. In essence, for individual subjects, by re-sampling 2,500 times from the data time series in each ROI, we created surrogate time series with the same mean, variance, autocorrelation function, and power spectrum as the data time series (Deshpande 2009; Kaminsk 2001; Kus 2004; Thieler et al., 1992). The resulting F values from GCA on these surrogate time series constituted the null hypothesis, which was tested against the data time series. G-causality was considered significant at $p<0.05$, corrected for false discovery rate, for individual connections (Genovese et al., 2001). Significance of G-causality was determined at the group level with a binomial test. The results confirmed connectivity between PMC as well as preSMA and the subcortical circuitry and the inter-connectivity between the IFC and preSMA (Fig. 2). Furthermore, the IFC did not show G-causality with the caudate or STN in either direction.

Psychophysiological interaction (PPI)

Figure 3 shows the brain regions that demonstrated greater connectivity with the IFC during stop success (SS) as compared to stop error (SE) trials, at a threshold of $p<0.005$, uncorrected and 10 voxels in the extent of activation. These brain regions included bilateral superior temporal, inferior frontal, and visual cortices, as well as a dorsomedial region in the superior frontal cortex (Table 2). To test our hypothesis specifically, we performed a region of interest analysis focusing on the preSMA with small volume correction. The results showed a significant cluster in the ROI: x=0, y=36, z=56, $p<0.05$, corrected for family-wise error (FWE) of multiple comparisons. At the same threshold (uncorrected $p<0.005$ and 10 voxels), a small cluster located in the region of ventromedial prefrontal cortex (x=16, y=48, z=−4, voxel Z=3.20, 15 voxels) showed a negative PPI.

In a previous study we showed greater preSMA activity in association with short as compared to long stop signal reaction time (SSRT, Li et al., 2006). Thus, to examine whether this functional connectivity between IFC and preSMA differs with respect to SSRT, we compared the effect sizes of this connectivity between subjects with short and long SSRT, on the basis of a median split (174 ± 23 ms vs. 235 ± 28 ms, $p<0.0001$, n=28 in each group). The results showed that the two groups did not differ in IFC-preSMA connectivity: 0.53 ± 0.93 vs. 0.31 ± 0.98 (p=0.217, one-tailed 2-sample t test). Comparison between subjects in the first and last quartiles of SSRT (157 ± 19 ms vs. 254 ± 29 ms, $p<0.0001$, n=14 in each group) yielded negative results: 0.30 ± 1.15 vs. 0.67 ± 1.02 (p=0.199, one-tailed 2-sample t test). We also failed to observe a correlation between the effect size of the IFC-preSMA connectivity with SSRT across all 57 subjects (r=0.053, p=0.688, Pearson regression).

Discussion

Our current findings from the Granger causality analyses showed that the primary motor cortex (PMC) and pre-supplementary motor area (preSMA) are functionally connected with the caudate head and subthalamic nucleus (STN). Furthermore, the inferior frontal cortex (IFC) is connected with the preSMA but not the caudate head or STN. Thus, with strong interconnectivity with the basal ganglia circuitry of motor control, the PMC and preSMA are in a position to engage the competition of go and stop processes, whereas the IFC indirectly influence the basal ganglia circuitry via projection to the preSMA. These new findings provide evidence differentiating the roles of the IFC and preSMA during stop signal inhibition. In particular, these data are inconsistent with the hypothesis of a hyperdirect pathway from the IFC to STN for motor inhibitory control (Aron and Poldrack, 2006).

The results from psychophysiologic interaction (PPI) analyses further corroborated this hypothesis: the IFC showed greater connectivity with the preSMA during stop success than during stop error trials. A number of other brain regions including the superior temporal and inferior frontal gyri as well as the visual cortices also showed a significant positive PPI. Although these findings were not specifically related to our hypothesis, they were consistent with many studies implicating these temporal/parietal structures in awareness and attentional binding of perceptual inputs (Campanella and Belin, 2007; Decety and Lamm, 2007; Driver and Mattingley, 1998; Linden, 2005; Redcay, 2008). Greater functional connectivity with temporal/parietal structures also appeared to be in accord with the relatively common finding of parietal activation in the literature of the no/no-go and stop signal task (Garavan et al., 2002; Karch et al., In press; Jaffard et al., 2008; Menon et al., 2001; Rubia et al., 2001). Greater connectivity with the visual cortices may underlie a mechanism of attentional enhancement of visual information processing (Brefczynski and DeYoe, 1999; Slotnick et al., 2003; Smith et al., 2000), and parietal activation might be the source of this striate cortical modulation (Poghosyan et al., 2005).

In earlier reports we demonstrated greater preSMA but not IFC activation (during stop success > stop error) in association with short as compared to long SSRT (Chao et al., In press; Li et al., 2006a). One question is whether the PPI between the IFC and preSMA is related to SSRT. Neither group-based comparison nor linear correlation showed a significant association between IFC-preSMA connectivity and SSRT. These results suggested that, although the IFC serves to detect the stop signal, the process of response suppression likely does not occur until the signal reaches the preSMA. This preliminary finding thus seems to further demarcate the roles of the IFC and preSMA during stop signal inhibition.

As described earlier, the IFC is part of the ventral attention system, which activates to the detection of a salient, behaviorally relevant target (see Corbetta and Shulman, 2002; Corbetta et al., 2008, for a review). In the stop signal task, the stop signal is both salient, because it is less frequent, and behaviorally relevant, because it demands a change of response. Thus, the saliency processing of the stop signal may explain greater IFC activation during stop (or no-go) trials as compared to go trials (Aron and Poldrack, 2006; Chevrier et al., 2007; Garavan et al., 1999; Konishi et al., 1999; Leung and Cai, 2007; Liddle et al., 2001; Rubia et al., 2003; Rubia et al., 2005; Xue et al., 2008). Many other studies have also provided evidence supporting a role of the IFC in target detection (Bledowski et al., 2004; Hampshire et al., 2007, 2009; Linden, 2005). In particular, Hampshire and colleagues showed that the IFC responds to target stimuli even when they were equated in frequency to the distractor stimuli, ruling out a surprise or “odd-ball” effect. Furthermore, by probing response only at the end of the stimulus sequence, the investigators demonstrated that response suppression was not required for this IFC activity to be observed. Thus, as suggested by Hampshire and colleagues, these findings support a role of the IFC in target detection during planned responses, in accord with the current results.

A recent study by Chikazoe et al. 2009 attempted to distinguish “odd-ball” from response inhibition activity by introducing infrequent “go” trials during a go/nogo task. They showed greater response in a posterior locus of the inferior frontal cortex during nogo as compared to infrequent go trials and suggested that this area is specifically related to response suppression. On the other hand, compared to an infrequent go response, a nogo response (no response) would likely require greater attentional processing to be successfully executed. For instance, one might speculate that while lapses of attention during nogo trials would prevent the “stop” process from being initiated in time, resulting in a nogo error, similar lapses during infrequent go trials would perhaps simply delay the go process. Thus, by contrasting successful nogo and infrequent go trials, one might be isolating neural processes directly related to attention. Nonetheless, the studies of Chizakoe and colleagues are interesting as they delineated inferior frontal subregions specialized for different aspects of go/nogo performance (Chizakoe et al., 2008; Hirose et al., in press).

How might one isolate the neural correlates of response inhibition during the stop signal task, independent of such attention-related activity? Previous work of Logan and colleagues provided a useful approach (Logan, 1994; Logan and Cowan, 1984). Logan and colleagues hypothesized in a model that the “go” and “stop” processes race to finish. The go process prepares and generates the movement while the stop process inhibits movement initiation: whichever process finishes first determines whether a response will be initiated or not. Importantly, the go and stop processes race toward the activation threshold independently. Thus, the time required for the stop signal to be processed so a response is withheld (i.e., stop signal reaction time or SSRT) can be computed on the basis of the go trial RT distribution and the odds of successful inhibits for different time delays between the go and stop signals. This is achieved by estimating the “critical” stop signal delay (SSD) at which a response can be correctly stopped in approximately 50% of the stop trials and subtracting the critical SSD from the median go trial RT (Logan, 1994). Generally speaking, the SSRT is the time required for a subject to cancel the movement after seeing the stop signal. Studies have used changes in SSRT as an index of the development of inhibitory control across life span (Bedard et al., 2002; Williams et al., 1999). A longer SSRT indicates poor response inhibition, and the wide behavioral literature of the stop signal task has employed prolonged SSRT as an index of impaired motor inhibitory control in patients with neurological or psychiatric conditions (Alderson et al., 2007; Bekker et al., 2005; Bellgrove et al., 2006; Gauggel et al., 2004; Huddy et al., 2008; Huizenga et al., 2009; Kooijmans et al., 2000; Li et al., 2006b; McAlonan et al., 2009; Rieger et al., 2003; Sagaspe et al., 2007).

Notably, our previous work suggested that the preSMA activity is inversely associated with the SSRT in individuals who did not differ in any other aspects of the stop signal performance (Chao et al., in press; Li et al., 2006a). This preSMA activity in inhibitory control is consistent with many previous studies suggesting functions of goal-directed action in this medial cortical structure (Boecker et al., 1998; Boecker et al., 2008; Brass and Haggard, 2007; de Jong and Paans, 2007; Lau et al., 2004; Leung and Cai, 2007; Mueller et al., 2007; Nachev et al., 2005; Nachev et al., 2007; Rushworth et al., 2002; Shima et al., 1996; Simmonds et al., 2008; Sumner et al., 2007; Suskauer et al., 2008). For instance, patients with preSMA lesions were impaired in inhibiting ongoing movements without showing changes in simple reaction time (Nachev et al., 2007). Such a role of preSMA in inhibitory motor control was also supported by electrophysiological studies. Stuphorn et al. showed that subthreshold electrical microstimulation of the presupplementary eye field improves inhibitory function (i.e., shortening SSRT) in macaque monkeys performing the stop signal task (Stuphorn and Schall, 2006). Electrical stimulation in the pre-SMA suppressed an automatic unwanted action while boosting a controlled desired action in macaque monkeys performing a “saccade-overriding” task (Isoda and Hikosaka, 2007).

Taken together, the current findings from GCA and PPI analyses suggested that both the IFC and preSMA are involved but play different roles during stop signal inhibition, with the IFC mediating attentional processing of the stop signal and the preSMA mediating motor inhibitory control. GCA has been a useful tool in describing effective connectivity between brain regions during fMRI of a cognitive task (Abler et al., 2006; Deshpande et al., 2008; Roebroeck et al., 2005; Stilla et al., 2007; Upadhyay et al., 2008). In particular, without a priori assumptions about the network connectivity, GCA is well suited for hypothesis testing. The present study set out to differentiate two hypotheses with one postulating direct connectivity between the IFC and STN and the other postulating a projection from the IFC to preSMA, which is connected with the basal ganglia circuitry. Our results clearly favored the latter hypothesis. On the other hand, one is cautioned against over-interpreting the patterns of connectivity. For instance, the current results could not be used to specify the individual roles of caudate nucleus and STN during stop signal inhibition.

To summarize, the current findings are inconsistent with the hypothesis of a hyperdirect pathway from the IFC to basal ganglia for inhibitory motor control. The results suggest that the IFC and preSMA play different roles in stop signal inhibition, with the IFC mediating attentional processing of the stop signal and the preSMA mediating response inhibition. The current findings have important implications for our understanding of the component processes of inhibitory control. In particular, deficits in stop signal inhibition have been implicated in many clinical conditions including attention deficit hyperactivity disorder and Parkinson's disease (Bush et al., 2005; McCloskey et al., 2005; Li and Sinha, 2008). These results would facilitate our understanding of the source of inhibitory control deficits in these illnesses.

Supplementary Material

Refer to Web version on PubMed Central for supplementary material.

Acknowledgments

This study was supported by NIH grants R01DA023248 (Li) and a Physician Scientist training grant (K12DA000167, Bruce Rounsaville). We thank Olivia Hendrick and Sarah Bednarski for editing the manuscript.

References

Abler B, Roebroeck A, Goebel R, Höse A, Schönfeldt-Lecuona C, Hole G, Walter H. Investigating directed influences between activated brain areas in a motor-response task using fMRI. Magn Reson Imaging 2006;24:181–185. [PubMed: 16455407]

Akaike H. A new look at the statistical model identification. Automatic Control. IEEE Transactions on 1974;19:716–723.

Alderson RM, Rapport MD, Kofler MJ. Attention-deficit/hyperactivity disorder and behavioral inhibition: a meta-analytic review of the stop-signal paradigm. J Abnorm Child Psychol 2007;35:745–758. [PubMed: 17668315]

Andersson JL, Hutton C, Ashburner J, Turner R, Friston K. Modeling geometric deformations in EPI time series. Neuroimage 2001;13:903–919. [PubMed: 11304086]

Aron AR, Poldrack RA. Cortical and subcortical contributions to Stop signal response inhibition: role of the subthalamic nucleus. J Neurosci 2006;26:2424–2433. [PubMed: 16510720]

Ashburner J, Friston KJ. Nonlinear spatial normalization using basis functions. Hum Brain Mapp 1999;7:254–266. [PubMed: 10408769]

Bedard AC, Nichols S, Barbosa JA, Schachar R, Logan GD, Tannock R. The development of selective inhibitory control across the life span. Dev Neuropsychol 2002;21:93–111. [PubMed: 12058837]

Bekker EM, Overtoom CC, Kenemans JL, Kooij JJ, De Noord I, Buitelaar JK, Verbaten MN. Stopping and changing in adults with ADHD. Psychol Med 2005;35:807–816. [PubMed: 15997601]

Bellgrove MA, Chambers CD, Vance A, Hall N, Karamitsios M, Bradshaw JL. Lateralized deficit of response inhibition in early-onset schizophrenia. Psychol Med 2006;36:495–505. [PubMed: 16336744]

Boecker H, Dagher A, Ceballos-Baumann AO, Passingham RE, Samuel M, Friston KJ, Poline J, Dettmers C, Conrad B, Brooks DJ. Role of the human rostral supplementary motor area and the basal ganglia in motor sequence control: investigations with $H_2^{15}O$ PET. J Neurophysiol 1998;79:1070–1080. [PubMed: 9463462]

Boecker H, Jankowski J, Ditter P, Scheef L. A role of the basal ganglia and midbrain nuclei for initiation of motor sequences. Neuroimage 2008;39:1356–1369. [PubMed: 18024158]

Brass M, Haggard P. To do or not to do: the neural signature of self-control. J Neurosci 2007;27:9141–9145. [PubMed: 17715350]

Brefczynski JA, DeYoe EA. A physiological correlate of the "spotlight" of visual attention. Nat Neurosci 1999;2:370–374. [PubMed: 10204545]

Brett, M.; Anton, J-L.; Valabregue, R.; Poline, J-P. Region of interest analysis using an SPM toolbox.. Abstract presented at the 8th International Conference on Functional Mapping of the Human Brain; Sendai, Japan. June 2-6; 2002.

Bush G, Valera EM, Seidman LJ. Functional neuroimaging of attention-deficit/hyperactivity disorder: a review and suggested future directions. Biol Psychiatry 2005;57:1273–1284. [PubMed: 15949999]

Campanella S, Belin P. Integrating face and voice in person perception. Trends Cogn Sci 2007;11:535–543. [PubMed: 17997124]

Chao HH-A, Luo X, Chang JL-K, Li C-SR. Greater activation of the anterior pre-supplementary motor area but not the inferior frontal cortex in association with short stop signal reaction time: an intrasubject analysis. BMC Neuroscience. In Press

Chevrier AD, Noseworthy MD, Schachar R. Dissociation of response inhibition and performance monitoring in the stop signal task using event-related fMRI. Hum Brain Mapp 2007;28:1347–1358. [PubMed: 17274022]

Chikazoe J, Jimura K, Asari T, Yamashita K, Morimoto H, Hirose S, Miyashita Y, Konishi S. Functional dissociation in right inferior frontal cortex during performance of go/no-go task. Cereb Cortex Jan; 2009 19(1):146–52. [PubMed: 18445602]

Corbetta M, Patel G, Shulman GL. The reorienting system of the human brain: from environment to theory of mind. Neuron 2008;58:306–324. [PubMed: 18466742]

Corbetta M, Shulman GL. Control of goal-directed and stimulus-driven attention in the brain. Nat Rev Neurosci 2002;3:201–215. [PubMed: 11994752]

de Jong BM, Paans AM. Medial versus lateral prefrontal dissociation in movement selection and inhibitory control. Brain Res 2007;1132:139–147. [PubMed: 17173869]

De Jong R, Coles MG, Logan GD, Gratton G. In search of the point of no return: the control of response processes. J Exp Psychol Hum Percept Perform 1990;16:164–182. [PubMed: 2137517]

Decety J, Lamm C. The role of the right temporoparietal junction in social interaction: how low-level computational processes contribute to meta-cognition. Neuroscientist 2007;13:580–593. [PubMed: 17911216]

Deshpande G, Hu X, Stilla R, Sathian K. Effective connectivity during haptic perception: a study using Granger causality analysis of functional magnetic resonance imaging data. Neuroimage 2008;40:1807–1814. [PubMed: 18329290]

Deshpande G, Laconte S, James GA, Peltier S, Hu X. Multivariate Granger causality analysis of fMRI data. Hum Brain Mapp 2009;30:1361–1373. [PubMed: 18537116]

Ding M, Bressler SL, Yang W, Liang H. Short-window spectral analysis of cortical event-related potentials by adaptive multivariate autoregressive modeling: data preprocessing, model validation, and variability assessment. Biol Cybern 2000;83(1):35–45. [PubMed: 10933236]

Driver J, Mattingley JB. Parietal neglect and visual awareness. Nat Neurosci 1998;1:17–22. [PubMed: 10195103]

Duvernoy, HM. The Human Brain: Surface, Blood Supply, and Three-Dimensional Sectional Anatomy. Vol. Second Edition. Springer Verlag; New York, NY: 1999.

Friston KJ, Ashburner J, Frith CD, Polone J-B, Heather JD, Frackowiak RSJ. Spatial registration and normalization of images. Hum Brain Mapp 1995a;2:165–189.

Friston KJ, Buechel C, Fink GR, Morris J, Rolls E, Dolan RJ. Psychophysiological and modulatory interactions in neuroimaging. Neuroimage 1997;6:218–229. [PubMed: 9344826]

Friston KJ, Holmes AP, Worsley KJ, Poline J-B, Frith CD, Frackowiak RSJ. Statistical parametric maps in functional imaging: a general linear approach. Hum Brain Mapp 1995b;2:189–210.

Garavan H, Ross TJ, Murphy K, Roche RA, Stein EA. Dissociable executive functions in the dynamic control of behavior: inhibition, error detection, and correction. Neuroimage 2002;17:1820–1829. [PubMed: 12498755]

Garavan H, Ross TJ, Stein EA. Right hemispheric dominance of inhibitory control: an event-related functional MRI study. Proc Natl Acad Sci USA 1999;96:8301–8306. [PubMed: 10393989]

Gauggel S, Rieger M, Feghoff TA. Inhibition of ongoing responses in patients with Parkinson's disease. J Neurol Neurosurg Psychiatry 2004;75:539–544. [PubMed: 15026491]

Genovese CR, Lazar NA, Nichols T. Thresholding of statistical maps in functional neuroimaging using the false discovery rate. Neuroimage 2002;15:870–878. [PubMed: 11906227]

Geweke J. Measurement of Linear Dependence and Feedback Between Multiple Time Series. J Am Stat Assoc 1982;77:304–313.

Gitelman DR, Penny WD, Ashburner J, Friston KJ. Modeling regional and psychophysiologic interactions in fMRI: the importance of hemodynamic deconvolution. Neuroimage 2003;19:200–207. [PubMed: 12781739]

Goebel R, Roebroeck A, Kim DS, Formisano E. Investigating directed cortical interactions in time-resolved fMRI data using vector autoregressive modeling and Granger causality mapping. Magn Reson Imaging 2003;21:1251–1261. [PubMed: 14725933]

Granger CWJ. Investigating Causal Relations by Econometric Models and Cross-spectral Methods. Econometrica 1969;37:424–438.

Hamilton, JD. Time Series Analysis. Princeton University Press; Princeton, NJ: 1994.

Hampshire A, Thompson R, Duncan J, Owen AM. Selective tuning of the right inferior frontal gyrus during target detection. Cogn Affect Behav Neurosci 2009;9:103–112. [PubMed: 19246331]

Hirose S, Chikazoe J, Jimura K, Yamashita KI, Miyashita Y, Konishi S. Sub-Centimeter Scale Functional Organization in Human Inferior Frontal Gyrus. Neuroimage. In press

Huddy VC, Aron AR, Harrison M, Barnes TR, Robbins TW, Joyce EM. Impaired conscious and preserved unconscious inhibitory processing in recent onset schizophrenia. Psychol Med 2008;16:1–10.

Huizenga HM, van Bers BM, Plat J, van den Wildenberg WP, van der Molen MW. Task complexity enhances response inhibition deficits in childhood and adolescent attention-deficit/hyperactivity disorder: a meta-regression analysis. Biol Psychiatry 2009;65:39–45. [PubMed: 18723163]

Hutton C, Bork A, Josephs O, Deichmann R, Ashburner J, Turner R. Image distortion correction in fMRI: A quantitative evaluation. Neuroimage 2002;16:217–240. [PubMed: 11969330]

Isoda M, Hikosaka O. Switching from automatic to controlled action by monkey medial frontal cortex. Nat Neurosci 2007;10:240–248. [PubMed: 17237780]

Jaffard M, Longcamp M, Velay JL, Anton JL, Roth M, Nazarian B, Boulinguez P. Proactive inhibitory control of movement assessed by event-related fMRI. Neuroimage 2008;42:1196–1206. [PubMed: 18588986]

Kamiński M, Ding M, Truccolo WA, Bressler SL. Evaluating causal relations in neural systems: granger causality, directed transfer function and statistical assessment of significance. Biol Cybern 2001;85:145–157. [PubMed: 11508777]

Karch S, Mulert C, Thalmeier T, Lutz J, Leicht G, Meindl T, Möller HJ, Jäger L, Pogarell O. The free choice whether or not to respond after stimulus presentation. Hum Brain Mapp. In press

Kincade JM, Abrams RA, Astafiev SV, Shulman GL, Corbetta M. An event-related functional magnetic resonance imaging study of voluntary and stimulus-driven orienting of attention. J Neurosci 2005;25:4593–4604. [PubMed: 15872107]

Konishi S, Nakajima K, Uchida I, Kikyo H, Kameyama M, Miyashita Y. Common inhibitory mechanism in human inferior prefrontal cortex revealed by event-related functional MRI. Brain 1999;122:981–991. [PubMed: 10355680]

Kooijmans R, Scheres A, Oosterlaan J. Response inhibition and measures of psychopathology: a dimensional analysis. Child Neuropsychol 2000;6:175–184. [PubMed: 11402395]

Kus R, Kaminski M, Blinowska KJ. Determination of EEG activity propagation: pair-wise versus multichannel estimate. IEEE Trans Biomed Eng 2004;51:1501–1510. [PubMed: 15376498]

Lau HC, Rogers RD, Haggard P, Passingham RE. Attention to intention. Science 2004;303:1208–1210. [PubMed: 14976320]

Leung HC, Cai W. Common and differential ventrolateral prefrontal activity during inhibition of hand and eye movements. J Neurosci 2007;27:9893–9900. [PubMed: 17855604]

Levitt H. Transformed up-down methods in psychoacoustics. J Acoust Soc Am 1970;49:467–477. [PubMed: 5541744]

Li C-SR, Huang C, Constable T, Sinha R. Imaging response inhibition in a stop signal task – neural correlates independent of signal monitoring and post-response processing. J Neurosci 2006a;26:186–192. [PubMed: 16399686]

Li C-SR, Huang C, Yan P, Paliwal P, Constable RT, Sinha R. Neural correlates of post-error slowing in a stop signal task. J Cognit Neurosci 2008a;20:1021–1029. [PubMed: 18211230]

Li C-SR, Milivojevic V, Kemp KA, Hong K, Sinha R. Performance monitoring and stop signal inhibition in abstinent patients with cocaine dependence. Drug Alcoh Depend 2006b;85:205–212.

Li CS, Sinha R. Inhibitory control and emotional stress regulation: neuroimaging evidence for frontal-limbic dysfunction in psycho-stimulant addiction. Neurosci Biobehav Rev 2008;32:581–597. [PubMed: 18164058]

Li C-SR, Yan P, Sinha R, Lee TW. The subcortical processes of motor response inhibition during a stop signal task. NeuroImage 2008b;41:1352–1363. [PubMed: 18485743]

Li C-SR, Yan P, Chao HH-A, Sinha R, Paliwal P, Constable RT, Lee TW, Zhang S. Error-specific medial cortical and subcortical activity during the stop signal task – a functional magnetic resonance imaging study. Neuroscience 2008c;155:1142–1151. [PubMed: 18674592]

Liddle PF, Kiehl KA, Smith AM. Event-related fMRI study of response inhibition. Hum Brain Mapp 2001;12:100–109. [PubMed: 11169874]

Linden DE. The p300: where in the brain is it produced and what does it tell us? Neuroscientist 2005;11:563–576. [PubMed: 16282597]

Linden DE, Prvulovic D, Formisano E, Völlinger M, Zanella FE, Goebel R, Dierks T. The functional neuroanatomy of target detection: an fMRI study of visual and auditory oddball tasks. Cereb Cortex 1999;9:815–823. [PubMed: 10601000]

Logan, GD. On the ability to inhibit thought and action: A user's guide to the stop signal paradigm.. Inhibitory Processes in Attention, Memory and Language. In: Dagenbach, D.; Carr, TH., editors. Academic Press; San Diego: 1994. 1994. p. 189-239.

Logan GD, Cowan WB. On the ability to inhibit thought and action: A theory of an act of control. Psychol Rev 1984;91:295–327.

McAlonan GM, Cheung V, Chua SE, Oosterlaan J, Hung SF, Tang CP, Lee CC, Kwong SL, Ho TP, Cheung C, Suckling J, Leung PW. Age-related grey matter volume correlates of response inhibition and shifting in attention-deficit hyperactivity disorder. Br J Psychiatry 2009;194:123–129. [PubMed: 19182173]

McCloskey MS, Phan KL, Coccaro EF. Neuroimaging and personality disorders. Curr Psychiatry Rep 2005;7:65–72. [PubMed: 15717989]

Menon V, Adleman NE, White CD, Glover GH, Reiss AL. Error-related brain activation during a Go/NoGo response inhibition task. Hum Brain Mapp 2001;12:131–143. [PubMed: 11170305]

Mueller VA, Brass M, Waszak F, Prinz W. The role of the preSMA and the rostral cingulate zone in internally selected actions. Neuroimage 2007;37:1354–1361. [PubMed: 17681798]

Nachev P, Kennard C, Husain M. Functional role of the supplementary and presupplementary motor areas. Nat Rev Neurosci 2008;9:856–869. [PubMed: 18843271]

Nachev P, Rees G, Parton A, Kennard C, Husain M. Volition and conflict in human medial frontal cortex. Curr Biol 2005;15:122–128. [PubMed: 15668167]

Nachev P, Wydell H, O'neill K, Husain M, Kennard C. The role of the presupplementary motor area in the control of action. Neuroimage 2007;36(Suppl 2):T155–63. [PubMed: 17499162]

Penny, W.; Holmes, AP. Random-effects analysis.. In: Frackowiak, et al., editors. Human Brain Function. Elsevier; San Diego: 2004. p. 843-850.

Poghosyan V, Shibata T, Ioannides AA. Effects of attention and arousal on early responses in striate cortex. Eur J Neurosci 2005;22:225–234. [PubMed: 16029212]

Redcay E. The superior temporal sulcus performs a common function for social and speech perception: implications for the emergence of autism. Neurosci Biobehav Rev 2008;32:123–142. [PubMed: 17706781]

Rieger M, Gauggel S, Burmeister K. Inhibition of ongoing responses following frontal, nonfrontal, and basal ganglia lesions. Neuropsychology 2003;17:272–282. [PubMed: 12803433]

Roebroeck A, Formisano E, Goebel R. Mapping directed influence over the brain using Granger causality and fMRI. Neuroimage 2005;25:230–242. [PubMed: 15734358]

Rubia K, Russell T, Overmeyer S, Brammer MJ, Bullmore ET, Sharma T, Simmons A, Williams SC, Giampietro V, Andrew CM, Taylor E. Mapping motor inhibition: conjunctive brain activations across different versions of go/no-go and stop tasks. Neuroimage 2001;13:250–261. [PubMed: 11162266]

Rubia K, Smith AB, Brammer MJ, Taylor E. Right inferior prefrontal cortex mediates response inhibition while mesial prefrontal cortex is responsible for error detection. Neuroimage 2003;20:351–358. [PubMed: 14527595]

Rubia K, Smith AB, Brammer MJ, Toone B, Taylor E. Abnormal brain activation during inhibition and error detection in medication-naïve adolescents with ADHD. Am J Psychiatry 2005;162:1067–1075. [PubMed: 15930054]

Rushworth MF, Hadland KA, Paus T, Sipila PK. Role of the human medial frontal cortex in task switching: a combined fMRI and TMS study. J Neurophysiol 2002;87:2577–2592. [PubMed: 11976394]

Sagaspe P, Philip P, Schwartz S. Inhibitory motor control in apneic and insomniac patients: a stop task study. J Sleep Res 2007;16:381–387. [PubMed: 18036083]

Sato JR, Junior EA, Takahashi DY, de Maria Felix M, Brammer MJ, Morettin PA. A method to produce evolving functional connectivity maps during the course of an fMRI experiment using wavelet-based time-varying Granger causality. Neuroimage 2006;31:187–196. [PubMed: 16434214]

Sato JR, Takahashi DY, Arcuri SM, Sameshima K, Morettin PA, Baccalá LA. Frequency domain connectivity identification: An application of partial directed coherence in fMRI. Hum Brain Mapp 2007;30:452–461. [PubMed: 18064582]

Serences JT, Shomstein S, Leber AB, Golay X, Egeth HE, Yantis S. Coordination of voluntary and stimulus-driven attentional control in human cortex. Psychol Sci 2005;16:114–122. [PubMed: 15686577]

Seth AK, Edelman GM. Distinguishing causal interactions in neural populations. Neural Comput 2007;19:910–933. [PubMed: 17348767]

Shima K, Mushiake H, Saito N, Tanji J. Role for cells in the presupplementary motor area in updating motor plans. Proc Natl Acad Sci (USA) 1996;93:8694–8698. [PubMed: 8710933]

Simmonds DJ, Pekar JJ, Mostofsky SH. Meta-analysis of Go/No-go tasks demonstrating that fMRI activation associated with response inhibition is task-dependent. Neuropsychologia 2008;46:224–232. [PubMed: 17850833]

Slotnick SD, Schwarzbach J, Yantis S. Attentional inhibition of visual processing in human striate and extrastriate cortex. Neuroimage 2003;19:1602–1611. [PubMed: 12948715]

Smith AT, Singh KD, Greenlee MW. Attentional suppression of activity in the human visual cortex. Neuroreport 2000;11:271–277. [PubMed: 10674469]

Stilla R, Deshpande G, LaConte S, Hu X, Sathian K. Posteromedial parietal cortical activity and inputs predict tactile spatial acuity. J Neurosci 2007;27:11091–11102. [PubMed: 17928451]

Stuphorn V, Schall JD. Executive control of countermanding saccades by the supplementary eye field. Nat Neurosci 2006;9:925–931. [PubMed: 16732274]

Sumner P, Nachev P, Morris P, Peters AM, Jackson SR, Kennard C, Husain M. Human medial frontal cortex mediates unconscious inhibition of voluntary action. Neuron 2007;54:697–711. [PubMed: 17553420]

Suskauer SJ, Simmonds DJ, Fotedar S, Blankner JG, Pekar JJ, Denckla MB, Mostofsky SH. Functional magnetic resonance imaging evidence for abnormalities in response selection in attention deficit hyperactivity disorder: differences in activation associated with response inhibition but not habitual motor response. J Cogn Neurosci 2008;20:478–493. [PubMed: 18004945]

Tseng YC, Li C-SR. The effects of response readiness and error monitoring on saccade countermanding. The Open Psychol J 2008;1:18–25.

Tzourio-Mazoyer N, Landeau B, Papathanassiou D, Crivello F, Etard O, Delcroix N, et al. Automated anatomical labeling of activations in SPM using a macroscopic anatomical parcellation of the MNI MRI single-subject. Neuroimage 2002;15:273–289. [PubMed: 11771995]

Upadhyay J, Silver A, Knaus TA, Lindgren KA, Ducros M, Kim DS, Tager-Flusberg H. Effective and structural connectivity in the human auditory cortex. J Neurosci 2008;28:3341–3349. [PubMed: 18367601]

Xue G, Aron AR, Poldrack RA. Common neural substrates for inhibition of spoken and manual responses. Cereb Cortex 2008;18:1923–1932. [PubMed: 18245044]

Verbruggen F, Logan GD. Response inhibition in the stop-signal paradigm. Trends Cogn Sci 2008;12:418–424. [PubMed: 18799345]

Wetherill GB, Chen H, Vasudeva RB. Sequential estimation of quantal response curves: A new method of estimation. Biometrika 1966;53:439–454.

Williams BR, Ponesse JS, Schachar RJ, Logan GD, Tannock R. Development of inhibitory control across the life span. Dev Psychol 1999;35:205–213. [PubMed: 9923475]

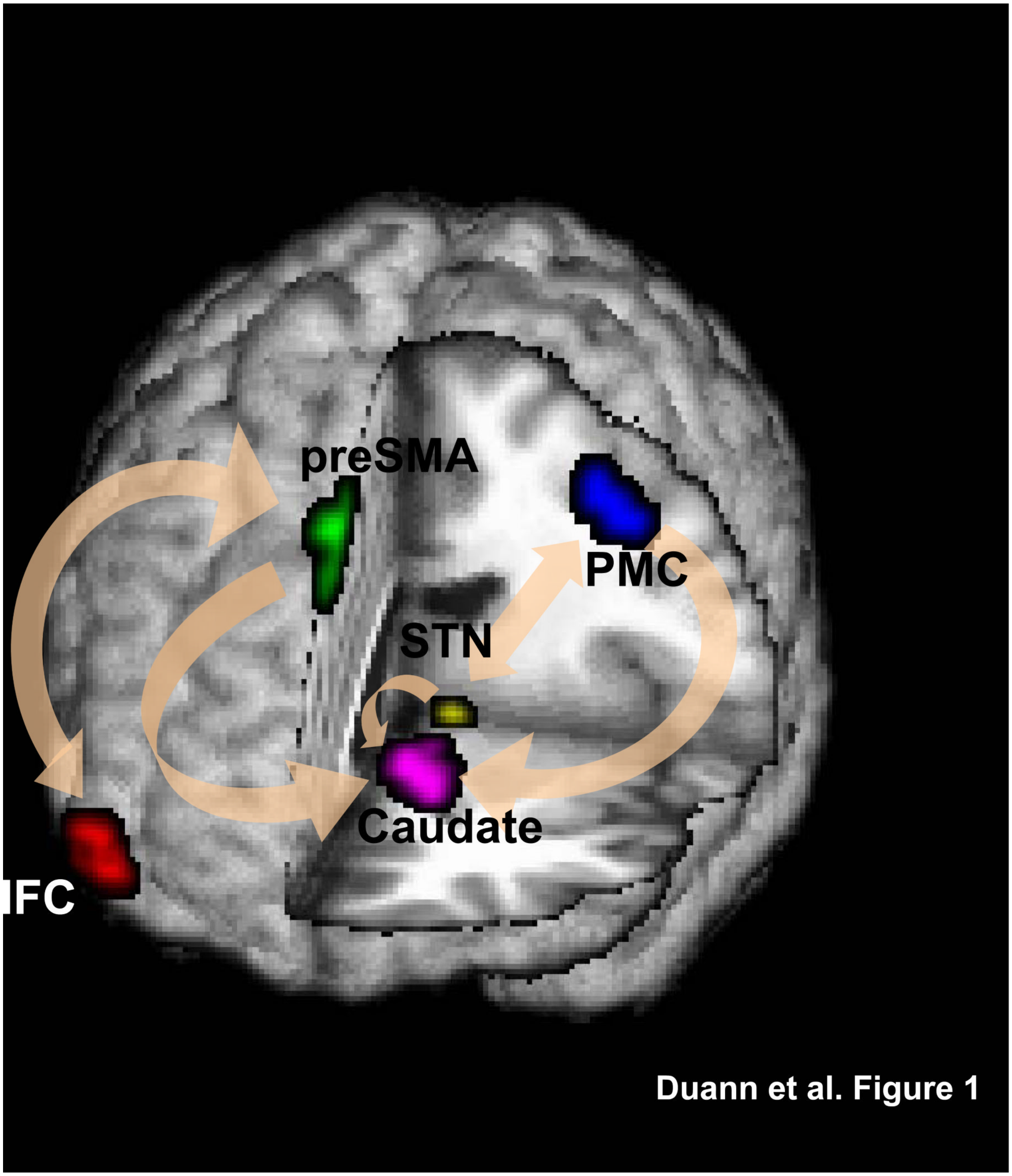

FIGURE 1.
The results of Granger (G-) causality analyses showed that the pre-supplementary motor area (preSMA) and primary motor cortex (PMC) are interconnected with the caudate head and the subthalamic nucleus (STN). The inferior frontal cortex (IFC) showed reciprocal G-causality with the preSMA but not with other structures.

NIH-PA Author Manuscript

NIH-PA Author Manuscript

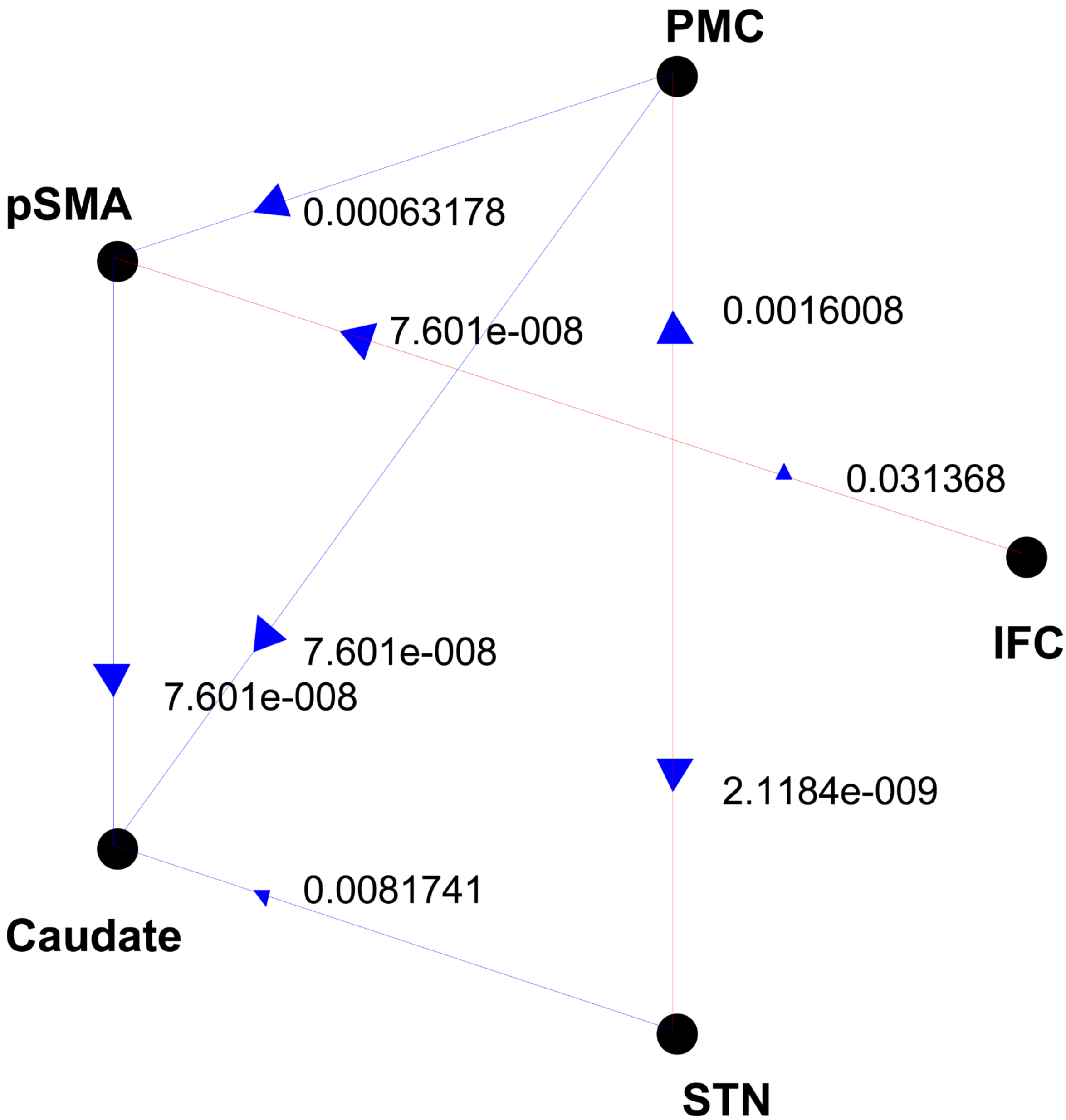

FIGURE 2.
The results of G-causality analysis with significance of individual connectivity tested against bootstrapped surrogate time series. P values are obtained from binomial test. Overall, the pattern of G-causality was almost identical to that shown in Figure 1.

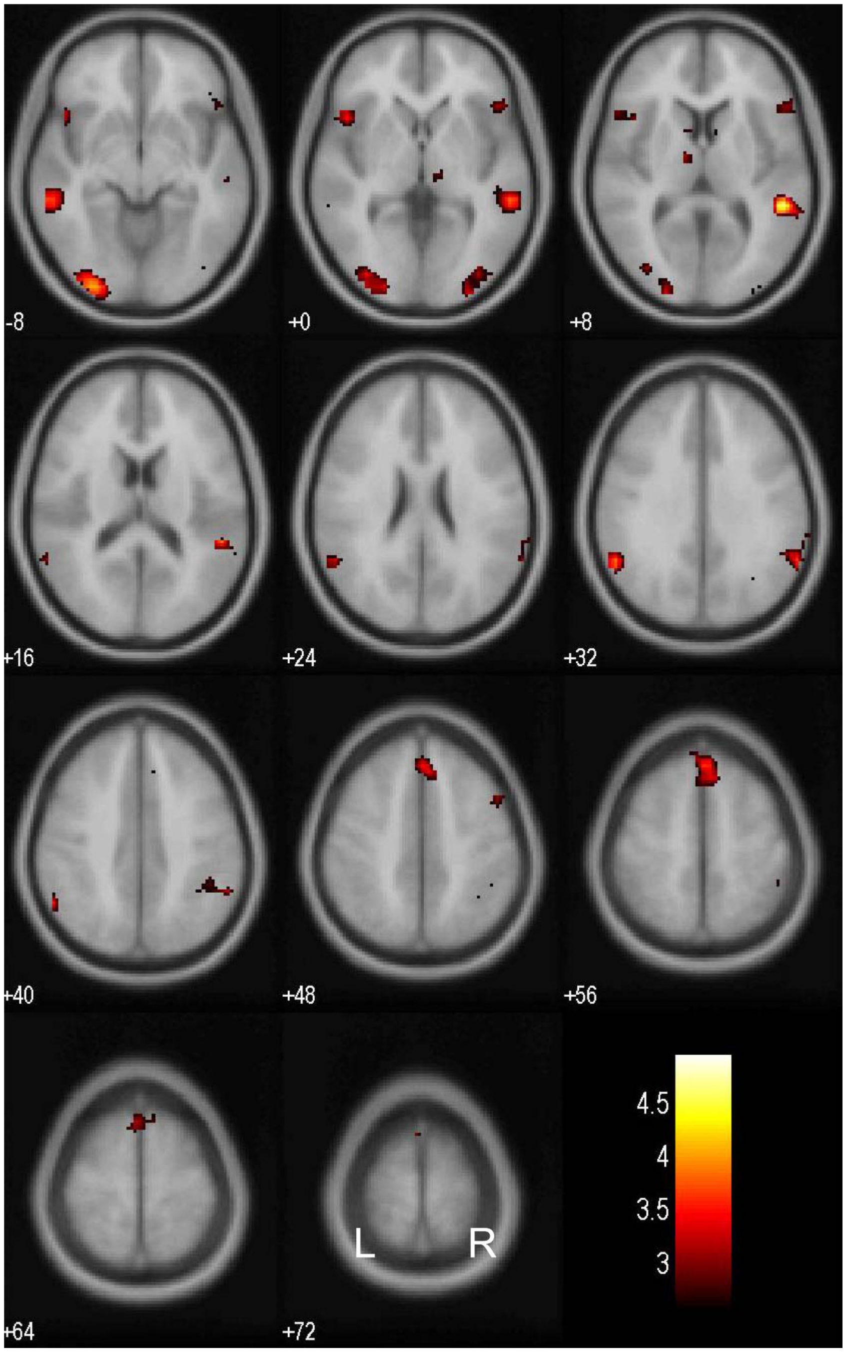

FIGURE 3.
Brain regions showing greater psychophysiologic interaction (PPI) with the inferior frontal cortex during stop success compared to stop error trials. BOLD contrast was overlaid on a T1 structural image in axial sections. Neurological orientation: right = right. Color bar represents voxel T value.

NIH-PA Author Manuscript
NIH-PA Author Manuscript

Table 1

Number of subjects showing significant Granger causality: stop signal task (a) and resting state (b) time series

(a)	**EFFECT**					
	IFC	**PMC**	**preSMA**	**Caudate**	**STN**	
CAUSE	**IFC**	28	48	24	19	
	PMC	34		37	49	50
	PreSMA	37	24		48	23
	Caudate	24	24	29		33
	STN	26	45	32	40	
(b)	**EFFECT**					
	IFC	**PMC**	**preSMA**	**Caudate**	**STN**	
CAUSE	**IFC**	2	5	5	3	
	PMC	2		3	6	8
	PreSMA	3	2		4	4
	Caudate	3	2	2		6
	STN	3	8	2	11	

Note: binomial test: n>38 for p<0.01 and n>36 for p<0.05, task data (n=57); n>21 for p<0.01 and n>19 for p<0.05, resting state data (n=30).

Table 2

Brain regions showing positive PPI

cluster size (voxels)	voxel Z value	MNI coordinate (mm)				Identified brain region
		x	y	z	Sidedness	
64	4.45	52	−40	12	R	superior/transverse temporal G
76	3.76	−32	−92	−8	L	occipital cortex
35	3.63	−56	−56	36	L	angular G
78	3.60	−4	16	68	L	superior frontal G
39	3.46	60	−52	32	R	angular G
21	3.45	−60	−36	−8	L	superior/transverse temporal G
30	3.37	−48	16	−4	L	inferior frontal G or anterior insula
25	3.16	40	32	−4	R	inferior frontal G
25	3.08	32	−96	4	R	occipital cortex

Note: $p<0.005$, uncorrected, and 10 voxels in spatial extent; G: gyrus